

# Correlation between the Atomic Alignment and the Alignment of XeX\* (B, C) Rotation in the Reactions of Oriented Xe ( $^3P_2$ , $M_J = 2$ ) + Halogen (X)-Containing Molecules

H. Ohoyama,\* K. Yasuda, and T. Kasai

Department of Chemistry, Graduate School of Science, Osaka University, Toyonaka, Osaka 560-0043, Japan

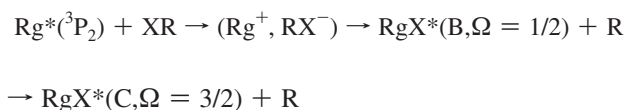
Received: July 7, 2009; Revised Manuscript Received: August 21, 2009

The polarization of the XeX\* (B) and XeX\* (C) emissions in the reactions of oriented Xe\* ( $^3P_2$ ,  $M_J = 2$ ) + halogen (X)-containing molecules (CCl<sub>4</sub>, CF<sub>3</sub>Br, CF<sub>3</sub>I, CH<sub>3</sub>I, NF<sub>3</sub>) has been measured as a function of each magnetic  $M_J'$  substate in the collision frame. The parallel polarization of the XeX\* (B, C) emissions to the relative velocity vector is commonly observed for all magnetic  $M_J'$  substates. The correlation between the atomic alignment ( $M_J'$ ) and the  $M_J'$ -dependent alignment ( $A^{M_J'}$ ) of the XeX\* (B, C) rotation is found to be extremely different between the XeX\* (B) and XeX\* (C) channels: For XeX\* (B),  $A^{M_J'}$  is highest for the  $M_J' = 0$  state, except CCl<sub>4</sub>, whereas the  $|M_J'| = 2$  states give the highest  $A^{M_J'}$  for XeX\* (C). Alternatively, the correlation between the configuration ( $L_Z'$ ) of the inner 5p orbital and the  $L_Z'$ -dependent alignment ( $A^{L_Z'}$ ) of the XeX\* (B, C) rotations is revealed. The collision with  $|L_Z'| = 1$  causes a similar positive alignment  $A^{L_Z'}$  for the XeX\* (B) and XeX\* (C) channels. The alignment  $A^{L_Z'}$  at the collision with  $|L_Z'| = 0$  is extremely different between the XeX\* (B) and XeX\* (C) channels. The collision with  $L_Z' = 0$  induces no alignment of XeX\* (C) except CF<sub>3</sub>I, that is,  $A^{L_Z'=0} \approx 0$ , whereas it induces the higher positive  $A^{L_Z'}$  of XeX\* (B). The different  $M_J'$  dependence on the alignment of the XeX\* (B, C) rotation between the XeX\* (B) and XeX\* (C) channels can be recognized as the change of reaction mechanism due to the difference in the favorable impact parameter for each  $M_J'$  state between the XeX\* (B) and XeX\* (C) channels, which reflects the  $\Omega'$  conservation in the course of ion-pair (Xe<sup>+</sup>–RX<sup>−</sup>) formation.

## 1. Introduction

The effect of reactant approach geometry on chemical reactions is an important field of dynamical stereochemistry.<sup>1–10</sup> The study on the reaction process involving aligned states of atoms is one of the well-explored fields in dynamical stereochemistry. For the naked outer atomic orbital prepared by optical pumping, the significant alignment dependences have been widely studied.<sup>11–14</sup> However, the direct interrogation of reactive geometric requirements for the multiplet atoms is difficult by optical pumping method, and little is known about the stereoselectivity on the triplet system such as metastable rare gas atoms Rg\* ( $np^5(n+1)s^1$ ), which have the unpaired inner atomic orbital shielded by the outer extended orbital.

The RgX\* formation in the reaction of Rg\*( $^3P$ ) with polyatomic halogen (X)-containing molecules RX has been widely studied as a benchmark system for the harpooning mechanism such as the formation of metal halide MX for the alkali–metal atoms.<sup>15–21</sup> Because the excited ion-pair potential  $V(\text{Rg}^+, \text{RX}^-)$  differs from that of the alkali metal atom case, the nonclosed shell nature of the positive ion-core Rg<sup>+</sup> with the spin–orbit coupling gives rise to two different excited rare gas halide product states, RgX\* (B) and RgX\* (C), that correlate with Rg<sup>+</sup> ( $^2P_{3/2}$ ) and X<sup>−</sup> ( $^1S_0$ ).<sup>21</sup>



X = halogen, R = any group

Generally speaking, it is expected that the configuration of the ion core of Rg\*( $^3P_2$ ) in the collision frame should play an important role in controlling the branching to each reaction channel. Despite the numerous studies on the RgX\* formation, however, the steric effect due to the nonclosed shell nature of the positive ion-core Rg<sup>+</sup> is still an unresolved problem.<sup>23,24</sup>

Recently, we have studied the atomic alignment effect for the RgX\* (B,  $\Omega = 1/2$ ) and RgX\* (C,  $\Omega = 3/2$ ) formations in the reactions of oriented Rg ( $^3P_2$ ,  $M_J = 2$ ) (Rg = Xe, Kr, Ar) with halogen (X)-containing molecules (RX).<sup>24</sup> We have reported that the reactant (RX) dependence of the atomic alignment effect is extremely different between the RgX\* (B) and RgX\* (C) channels. (For the RgX\* (C) channel, an analogous atomic alignment effect is commonly observed despite the difference of RX and Rg. In contrast, for the RgX\* (B) channel, the atomic alignment effect shows a diverse dependence on RX and Rg). To explain these atomic alignment effects, we have proposed an  $\Omega'$  conservation model in which the angular momentum  $\Omega'$  of the Rg<sup>+</sup> ion core of Rg ( $^3P_2$ ) in the collision frame is assumed to be conserved in the course of ion-pair (Rg<sup>+</sup>–RX<sup>−</sup>) formation. According to this model, we have suggested that the atomic alignment effect for the excimer formation is dominantly controlled by the rotational coupling

\* Corresponding author.

of the angular momentum  $\Omega'$  due to the change of quantization axis from collision frame ( $\Omega'$ ) to the ion-pair ( $\text{Rg}^+-\text{RX}^-$ ) frame ( $\Omega_{\text{I}}$ ). In particular, the atomic alignment effect for the  $\text{RgX}^*$  (C,  $\Omega = 3/2$ ) formation can be explained by only the rotational coupling through the ion-pair ( $\text{Rg}^+-\text{RX}^-$ ) formation. The collision under the  $|M_J| = 2$  configurations of  $\text{Rg}(^3\text{P}_2)$  with a small impact parameter is exceptionally reactive for the  $\text{RgX}^*$  (B,  $\Omega = 1/2$ ) formation without the conservation of the  $\Omega_{\text{I}}$  component in the ion-pair ( $\text{Rg}^+-\text{RX}^-$ ) frame. Although the proposed model can explain the atomic alignment effect for the  $\text{RgX}^*$  (B,  $\Omega = 1/2$ ) and  $\text{RgX}^*$  (C,  $\Omega = 3/2$ ) formations well, there is no proof that  $\Omega'$  is really conserved in the course of  $\text{RgX}^*$  formation. To make clear whether  $\Omega'$  is conserved in the course of  $\text{RgX}^*$  formation, it is of great important to know the correlation between the alignment of  $\text{RgX}^*$  rotation and the atomic alignment ( $M_J$ ) because such experiments give particularly detailed information on the disposal of angular momentum in reactive collisions. In particular, it is expected that the  $\Omega'$  conservation should cause the difference in the alignment of  $\text{RgX}^*$  rotation between the  $\text{RgX}^*$  (B) and  $\text{RgX}^*$  (C) channels because the alignment of  $\text{RgX}^*$  rotation should be affected by the difference in the favorable impact parameter for each  $M_J$  state between the  $\text{RgX}^*$  (B) and  $\text{RgX}^*$  (C) channels.

The alignment of products from reactive collision has been studied since the early 1970s.<sup>25</sup> The Legendre moment  $\langle P_2(\hat{j} \cdot \hat{v}_R) \rangle$  has been determined as a function not only of collision energy<sup>26,27</sup> but also of reagent molecule orientation<sup>14,28,29</sup> and product internal states.<sup>30-33</sup> (Here  $\hat{j}$  is the unit vector corresponding to the product rotational angular momentum,  $\vec{j}$ , and  $\vec{v}_R$  is the unit vector corresponding to the relative velocity  $\vec{v}_R$ ). For the reactions of Xe ( $^3\text{P}_{0,2}$ ) with halogenated methanes, Martin et al. have studied the  $\text{XeX}^*$  rotational alignment as a function of collision energy.<sup>34</sup> Unfortunately, however, their study gives no information on how the unpaired inner orbital of  $\text{Xe}^*$  plays a role in the  $\text{XeX}^*$  rotational alignment.

In the present study, we studied the correlation between the atomic alignment  $M_J$  and the alignment of  $\text{XeX}^*$  (B, C) rotations in the oriented Xe ( $^3\text{P}_2$ ) + RX  $\rightarrow$   $\text{XeX}^*$  (B, C) + R reactions (RX =  $\text{CCl}_4$ ,  $\text{CF}_3\text{Br}$ ,  $\text{CF}_3\text{I}$ ,  $\text{CH}_3\text{I}$ ,  $\text{NF}_3$ ). It was found that the correlation between the atomic alignment  $M_J$  and the alignment of  $\text{XeX}^*$  (B, C) rotations is extremely different between the  $\text{XeX}^*$  (B) and  $\text{XeX}^*$  (C) channels.

## 2. Experimental Section

Details of the experimental apparatus and the procedure are described elsewhere.<sup>35,36</sup> In brief, we generated a pure Xe ( $^3\text{P}_2$ ,  $M_J = 2$ ) atomic beam by using an inhomogeneous magnetic hexapole. An RX molecular beam (RX:  $\text{CCl}_4$ ,  $\text{CF}_3\text{Br}$ ,  $\text{CF}_3\text{I}$ ,  $\text{CH}_3\text{I}$ ,  $\text{NF}_3$ ) was injected from a pulsed valve with a stagnation pressure of 10 Torr. In a homogeneous magnetic orientation field  $\mathbf{B}$ , the  $M_J$  state-selected Xe ( $^3\text{P}_2$ ,  $M_J = 2$ ) atomic beam collides with the RX molecular beam. The emission from each product,  $\text{XeX}^*$  (B) and  $\text{XeX}^*$  (C), is selected by a suitable band-pass filter and detected by a cooled and magnetic shielded photomultiplier (Hamamatsu R943-02) mounted at 30 cm apart from the beam crossing point. The emission was viewed at right angle through a polarizer (SIGMA KOKI, SPF-30C-32). The polarizer was set at two positions: The parallel configuration ( $\Phi_{\parallel}$ ) passes the light polarized along the relative velocity ( $v_R$ ), and the perpendicular configuration ( $\Phi_{\perp}$ ) passes the light polarized perpendicular to  $v_R$ . The emission of  $\text{XeX}^*$  (B, C) was measured as a function of the direction of the magnetic orientation field  $\mathbf{B}$  in the laboratory frame (angle  $\Theta$ ). The

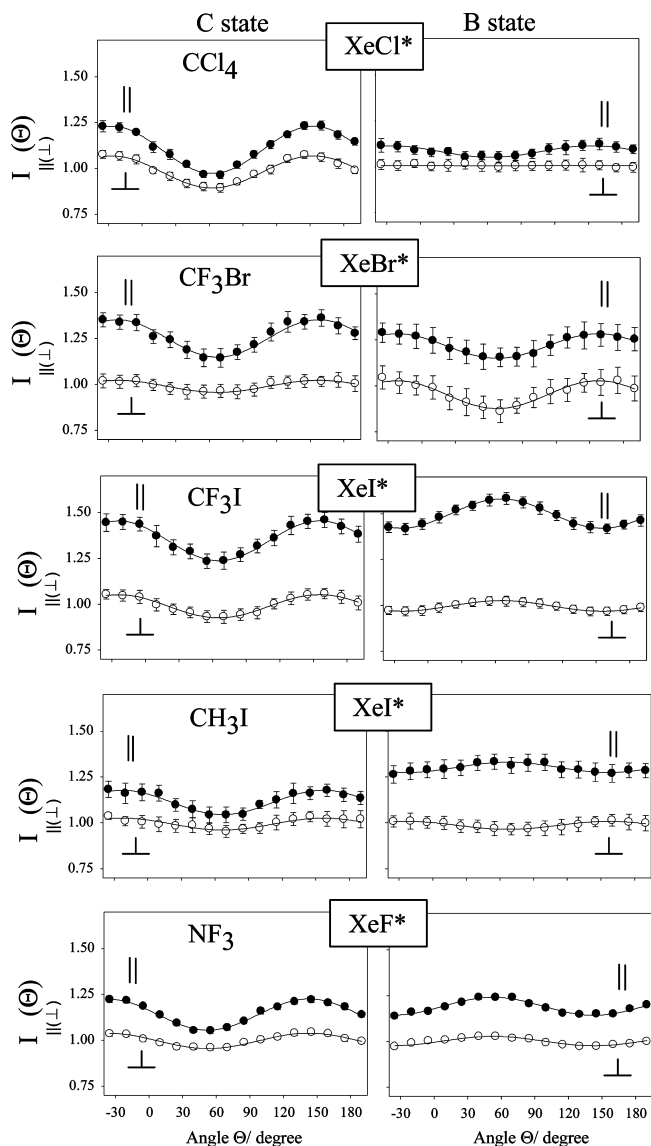


**Figure 1.** Emission intensities of  $\text{XeX}^*$  (B, C),  $I_{\parallel,\perp}(\Theta)$ , as a function of the magnetic orientation field direction  $\Theta$  at two polarization conditions  $\Phi_{\parallel}$  (●) and  $\Phi_{\perp}$  (○). The longitudinal axis was scaled by the intensity of  $I_{\perp}(\Theta)$  averaged over  $\Theta$  (i.e., the  $a_0^+$  coefficient in eq 2). The  $\Theta$  dependences reproduced by eq 3 are shown as the solid lines.

magnetic orientation field was rotated around the beam crossing point over the angular range  $-45 \leq \Theta \leq 165^\circ$  by an interval of  $15^\circ$ . The origin of  $\Theta$  is the direction of the Xe ( $^3\text{P}_2$ ,  $M_J = 2$ ) beam velocity vector. The signal from the photomultiplier was counted by a multichannel scaler (Stanford SR430).

## 3. Results and Discussion

**3.1. Atomic Alignment Effect for the Polarization of  $\text{XeX}^*$  (B, C) Emission.** For the Xe ( $^3\text{P}_2$ ,  $M_J = 2$ ) + RX reactions, the emission intensity  $I_{\parallel,\perp}(\Theta)$  from the products  $\text{XeX}^*$  (B, C) was measured under two polarization conditions ( $\Phi_{\parallel}$  and  $\Phi_{\perp}$ ) as a function of the orientation field direction  $\Theta$ . The  $\Theta$  dependences of the  $\text{XeX}^*$  (B, C) emissions at two polarization conditions,  $I_{\parallel}(\Theta)$  and  $I_{\perp}(\Theta)$ , are shown in Figure 1. A significant parallel polarization of  $\text{XeX}^*$  (B, C) emissions with respect to the relative velocity vector is observed for all reaction systems. We can observe a notable difference between  $I_{\parallel}(\Theta)$  and  $I_{\perp}(\Theta)$

in both the intensity and the  $\Theta$  dependence. These differences show that atomic alignment plays an important role in the alignment of the product rotation.

In the present study, the Xe ( $^3P_2$ ,  $M_J = 2$ ) atomic beam is oriented in a homogeneous magnetic orientation field,  $\mathbf{B}$ . For the collision processes, however, the relative velocity vector serves as the other relevant quantization axis. The cross section is then a function of the angle between those two quantization axes. In the following discussion, we use the notation of  $M_J$  for projections in the laboratory frame (the quantization axis is the magnetic orientation field,  $\mathbf{B}$ ). Primed symbols such as  $M_J'$  and  $\Omega'$  are used for projections in the collision frame. (The quantization axis is the relative velocity vector.)

**3.2.  $M_J'$ -Dependent Cross Section at Each Polarization,  $\sigma_{\parallel,(\perp)}^{M_J'}$ .** To extract the quantitative information on the steric effect, we accommodate the evolution procedure based on an irreducible representation of the density matrix. The detail of the analytical procedures and the derivation of all the algebra are reported elsewhere.<sup>35</sup> The  $\Theta$  dependence of the emission intensity at each polarization,  $I_{\parallel,(\perp)}(\Theta)$ , can be simplified as the following equation using the relative cross sections,  $\sigma_{\parallel,(\perp)}^{M_J'}$ , in the collision frame

$$I_{\parallel,(\perp)}(\Theta) = \frac{1}{280}(39\sigma_{\parallel,(\perp)}^{M_J'=0} + 88\sigma_{\parallel,(\perp)}^{M_J'=1} + 153\sigma_{\parallel,(\perp)}^{M_J'=2}) + \frac{1}{16}(-3\sigma_{\parallel,(\perp)}^{M_J'=0} - 4\sigma_{\parallel,(\perp)}^{M_J'=1} + 7\sigma_{\parallel,(\perp)}^{M_J'=2}) \cos 2(\Theta_{v_R} - \Theta) + \frac{1}{64}(3\sigma_{\parallel,(\perp)}^{M_J'=0} - 4\sigma_{\parallel,(\perp)}^{M_J'=1} + \sigma_{\parallel,(\perp)}^{M_J'=2}) \cos 4(\Theta_{v_R} - \Theta) \quad (1)$$

where  $\Theta_{v_R}Z$  is the direction of relative velocity,  $v_R$ , in the laboratory coordinate. Because this angle has a distribution by the misalignment caused by the velocity distribution of the RX molecular beam, we must use the  $\cos 2n(\Theta_{v_R} - \Theta)$  factors averaged over the Maxwell–Boltzmann velocity distribution of the RX molecular beam at room temperature,  $\langle \cos(2n(\Theta_{v_R} - \Theta)) \rangle$ . This equation is equivalent to the following multipole moment form

$$I_{\parallel,(\perp)}(\Theta) = a_0^{\parallel,(\perp)} + a_2^{\parallel,(\perp)} \langle \cos(2(\Theta_{v_R} - \Theta)) \rangle + a_4^{\parallel,(\perp)} \langle \cos(4(\Theta_{v_R} - \Theta)) \rangle \quad (2)$$

As a whole, it was found that no notable  $a_4$  term is recognized for all reaction systems, indicating that the excimer formation is dominantly controlled by the alignment of the inner 5p electron of Xe ( $^3P_2$ ,  $M_J = 2$ ) in the collision frame. Therefore, the parameters,  $a_2^{\parallel,(\perp)}/a_0^{\parallel,(\perp)}$ , can be determined by the fitting of  $I_{\parallel,(\perp)}(\Theta)$  using eq 3 through a  $\chi^2$  analysis

$$I_{\parallel,(\perp)}(\Theta) = a_0^{\parallel,(\perp)} + a_2^{\parallel,(\perp)} \langle \cos 2(\Theta_{v_R} - \Theta) \rangle \quad (3)$$

The resultant parameters  $a_2^{\parallel,(\perp)}/a_0^{\parallel,(\perp)}$  were shown in Figure 2. It is found that the reactant (RX) dependence of the atomic alignment effect is extremely different between the XeX\* (B) and XeX\* (C) channels. For XeX\* (C), an analogous atomic alignment effect is commonly observed despite the difference between RX. In contrast, the atomic alignment effect shows a diverse dependence on RX for XeX\* (B). A similar result has been reported in our previous study on the atomic alignment effect without polarization analysis.<sup>24</sup>

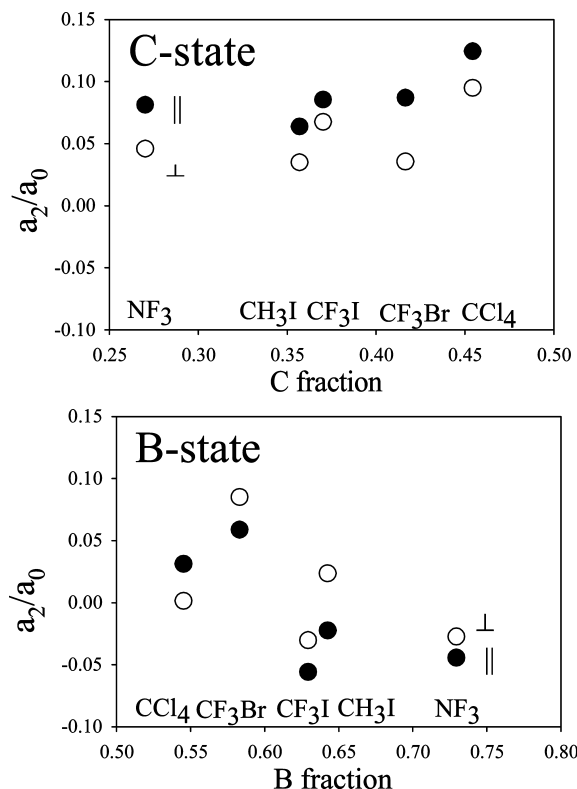


**Figure 2.**  $a_2^{\parallel,(\perp)}/a_0^{\parallel,(\perp)}$  parameters determined by the fitting of  $I_{\parallel,(\perp)}(\Theta)$  using eq 3 under the two polarization conditions:  $\Phi_{\perp}$  (●) and  $\Phi_{\parallel}$  (○). The errors for  $a_2^{\parallel,(\perp)}/a_0^{\parallel,(\perp)}$  are typically less than  $\pm 0.005$ . The abscissa axis is the branching fraction for each XeX\* (B, C) channel, which is cited from refs 15–21.

It is found that  $a_2^{\parallel}/a_0^{\parallel}$  is larger than  $a_2^{\perp}/a_0^{\perp}$  for XeX\* (C), whereas,  $a_2^{\perp}/a_0^{\perp}$  is larger than  $a_2^{\parallel}/a_0^{\parallel}$  for XeX\* (B) except for CCl<sub>4</sub>.

**3.3.  $M_J'$ -Dependent Alignment,  $A^{M_J'}$ .** The cross sections  $\sigma_{\parallel,(\perp)}^{M_J'}$  can be derived from the experimental coefficient ratios  $a_2^{\parallel,(\perp)}/a_0^{\parallel,(\perp)}$  in Figure 2. They were shown in Figure 3A. An extremely different  $M_J'$  dependence of  $\sigma_{\parallel,(\perp)}^{M_J'}$  is recognized between the XeX\* (C) and XeX\* (B) channels. For the XeX\* (C) channel, it is found that  $\sigma_{\parallel,(\perp)}^{M_J'=2}$  is the largest and  $\sigma_{\parallel,(\perp)}^{M_J'=0}$  is the smallest for all reaction systems. In contrast, the magnitude correlation among  $\sigma_{\parallel,(\perp)}^{M_J'}$  shows a diverse dependence on RX for the RgX\* (B) channel. The CCl<sub>4</sub> and CF<sub>3</sub>Br systems have a similar correlation to that for the XeX\* (C) channel. For the CF<sub>3</sub>I and NF<sub>3</sub> systems,  $\sigma_{\parallel,(\perp)}^{M_J'=0}$  is the largest and  $\sigma_{\parallel,(\perp)}^{M_J'=2}$  is the smallest. CH<sub>3</sub>I shows an opposite magnitude correlation between the different polarization conditions:  $\Phi_{\parallel}$  and  $\Phi_{\perp}$ .

On the basis of  $\sigma_{\parallel,(\perp)}^{M_J'}$  under each polarization condition, we can determine the  $M_J'$ -dependent alignment ( $A^{M_J'}$ ) for the product angular momentum  $j$  to the relative velocity  $v_R$  as follows<sup>25</sup>

$$A^{M_J'} = -2 \langle P_2(\hat{j} \cdot v_R) \rangle_{M_J'} = 4(\sigma_{\parallel}^{M_J'} - \sigma_{\perp}^{M_J'}) / (\sigma_{\parallel}^{M_J'} + 2\sigma_{\perp}^{M_J'}) \quad (4)$$

They were plotted in Figure 3B. The correlation between  $A^{M_J'}$  and  $M_J'$  is significantly different between the XeX\* (B) and XeX\* (C) channels except for CCl<sub>4</sub>. For the XeX\* (B) channel,  $A^{M_J'}$  is largest for the  $M_J' = 0$  state, whereas, the  $|M_J'| = 2$  states give the largest  $A^{M_J'}$  in the XeX\* (C) channel. For CCl<sub>4</sub>, the  $|M_J'| = 2$  states give the largest  $A^{M_J'}$  in both the XeX\* (C) and XeX\* (B) channels. These differences strongly suggest that the atomic alignment ( $M_J'$ ) of Xe ( $^3P_2$ ,

$M_j = 2$ ) in the collision frame should make a difference on the reaction mechanism between the  $\text{XeX}^*$  (B) and  $\text{XeX}^*$  (C) channels.

**3.4.  $L_z'$ -Dependent Alignment,  $A^{L_z'}$ .** As mentioned above, no notable  $a_4$  term is recognized for all reaction systems. The minor contribution of rank 4 moment ( $a_4$ ) directly signifies that  $J (= 2)$  is not the proper quantum number to describe the essential dynamics of the present system. Rather, the physics of the process is dominantly determined by the orbital angular momentum  $L (= 1)$  and its components  $L_z'$  in the collision frame.<sup>35</sup> In such a case, the cross section  $\sigma_{\parallel(\perp)}^{M_j'$  can be alternatively expressed by the cross section  $\sigma_{\parallel(\perp)}^{L_z'}$  on the basis of the  $|L, S, L_z', S_z'\rangle$  basis using a standard recoupling procedure through the Clebsch–Gordan coefficients.<sup>35,37</sup> Because the  $S_z'$  and the sign of  $L_z'$  give no effect for the reactivity, the  $\sigma_{\parallel(\perp)}^{M_j'}$  can be directly related to  $\sigma_{\parallel(\perp)}^{L_z'}$  by

$$\begin{aligned}\sigma_{\parallel(\perp)}^{M_j'=2} &= \sigma_{\parallel(\perp)}^{L_z'=1} \\ \sigma_{\parallel(\perp)}^{M_j'=1} &= \frac{1}{2} \times \sigma_{\parallel(\perp)}^{L_z'=1} + \frac{1}{2} \times \sigma_{\parallel(\perp)}^{L_z'=0} \\ \sigma_{\parallel(\perp)}^{M_j'=0} &= \frac{1}{3} \times \sigma_{\parallel(\perp)}^{L_z'=1} + \frac{2}{3} \times \sigma_{\parallel(\perp)}^{L_z'=0}\end{aligned}\quad (5)$$

By using  $\sigma_{\parallel(\perp)}^{L_z'}$ , we can alternatively define the  $L_z'$ -dependent alignment ( $A^{L_z'}$ ) for the product angular momentum  $j$  to the relative velocity  $v_R$  by

$$A^{L_z'} = -2\langle P_2(\hat{j} \cdot v_R) \rangle_{L_z'} = 4(\sigma_{\parallel}^{L_z'} - \sigma_{\perp}^{L_z'}) / (\sigma_{\parallel}^{L_z'} + 2\sigma_{\perp}^{L_z'}) \quad (6)$$

They were shown in Figure 4 as a function of the rate constant for  $\text{XeX}^*$  formation. It is found that the alignment of the product

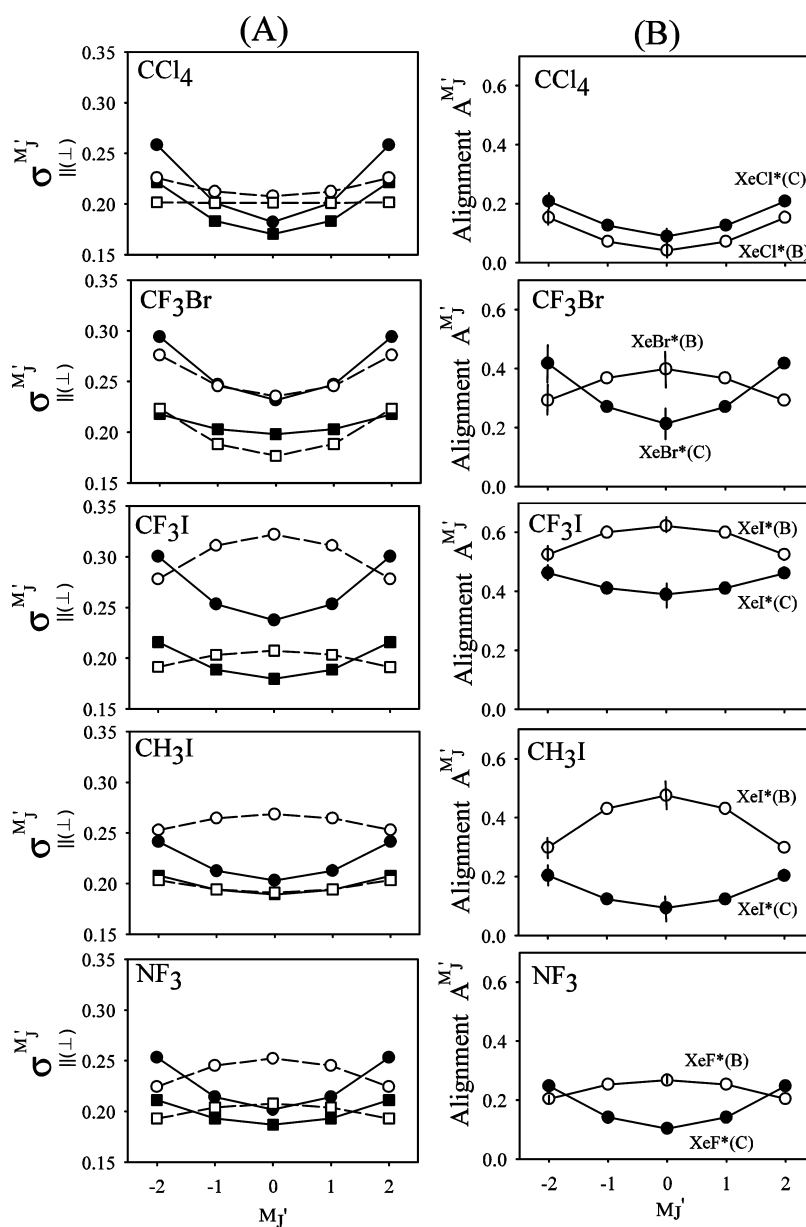


**Figure 3.** (A)  $M_j'$ -dependent cross section  $\sigma_{\parallel(\perp)}^{M_j'}$  for the  $\text{XeX}^*$  (C) (closed symbols) and  $\text{XeX}^*$  (B) (open symbols) channels under two polarization conditions:  $\Phi_{\parallel}$  (circle) and  $\Phi_{\perp}$  (square). The errors for  $\sigma_{\parallel(\perp)}^{M_j'}$  are estimated to be less than  $\pm 0.01$  from the law of propagation of errors. (B)  $M_j'$ -dependent alignment parameters  $A^{M_j'}$  for the product angular momentum  $j$  to the relative velocity  $v_R$  for the  $\text{XeX}^*$  (C) (●) and  $\text{XeX}^*$  (B) (○) channels. The estimated errors are shown for  $A^{M_j'=2}$  and  $A^{M_j'=0}$  as the references.



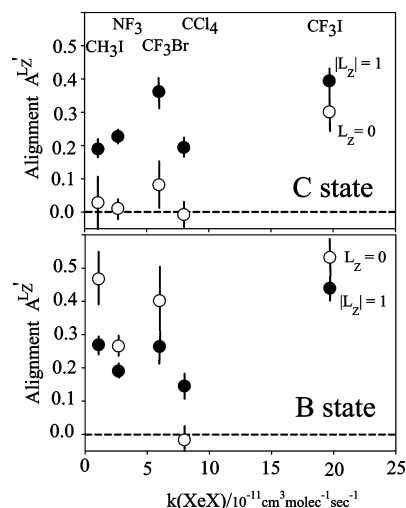


**Figure 4.**  $L_{z'}$ -dependent alignment parameters  $A^{L_{z'}}$  at the two configurations of the 5p orbital ( $L_{z'}$ ) of Xe ( $^3P_2$ ,  $M_j = 2$ ) in the collision frame:  $|L_{z'}| = 1$  (●),  $L_{z'} = 0$  (○). The errors for  $A^{L_{z'}}$  were estimated from the standard law of propagation of errors. The abscissa axis is the rate constant for XeX\* formation, which is cited from refs 15–21.

angular momentum  $j$  strongly depends on the configuration ( $L_{z'}$ ) of the 5p orbital in the collision frame. As a whole, the collision with  $|L_{z'}| = 1$  causes a similar positive alignment  $A^{L_{z'}}$  for the XeX\* (B) and XeX\* (C) channels. On the other hand, the alignment ( $A^{L_{z'}}$ ) at the collision with  $L_{z'} = 0$  is extremely different between the XeX\* (B) and XeX\* (C) channels. The collision with  $L_{z'} = 0$  induces no alignment for XeX\* (C), that is,  $A^{L_{z'}=0} \approx 0$ , whereas, it causes the higher positive alignment for XeX\* (B) as compared with that at the collision with  $|L_{z'}| = 1$ . These results strongly suggest that the reaction mechanism is switched by the configuration ( $L_{z'}$ ) of 5p orbital in the collision frame.

**3.5. Comparison with the  $\Omega'$ -Conservation Model.** In the  $\Omega'$ -conservation model,<sup>24</sup> the angular momentum  $\Omega'$  of the Xe<sup>+</sup> ( $^2P_{3/2}$ ) ion core in each Xe ( $^3P_2$ ,  $M_j'$ ) state in the collision frame is assumed to be preserved into the configuration of the hole in the 5p shell of Xe<sup>+</sup> ( $^2P_{3/2}$ ) in the ion pair (Xe<sup>+</sup>–RX<sup>−</sup>) in the collision frame at the distance  $R_{ET}$ , where the ion pair is formed via the 6s electron transfer. In addition, the cross section for the XeX\* ( $\Omega$ ) formation is assumed to be controlled by the  $\Omega_I$  component in the ion pair (Xe<sup>+</sup>( $^2P_{3/2}$ )–RX<sup>+</sup>) frame that is determined by the nonadiabatic switching of the quantization axis (i.e., rotational coupling) from the collision frame to the ion pair (Xe<sup>+</sup>( $^2P_{3/2}$ )–RX<sup>+</sup>) frame (i.e., the electrostatic field along the ion pair axis) at the distance  $R_{ET}$ .

According to the  $\Omega'$  conservation in the course of ion-pair formation, the fraction of  $\Omega'$  component in each Xe( $^3P_2$ ,  $M_j'$ ) state,  $W_{\Omega'}(M_j')$ , can be calculated by using a standard recoupling procedure of angular momentum in terms of the Clebsch–Gordan coefficients for the case of  $J = 2$ ,  $j = 3/2$  (for the ion core), and  $s = 1/2$  (for the 6s electron) as follows<sup>37</sup>

$$W_{\Omega'}(M_j') = | \langle 2, M_j' | 3/2, \Omega' = (M_j' - m_s'), 1/2, m_s' \rangle |^2 \quad (7)$$

Because the Xe<sup>+</sup>( $^2P_{3/2}$ ) core has two spin–orbit states,  $\Omega' = 3/2$  and  $\Omega' = 1/2$ , in the collision frame, the  $M_j'$ -dependent cross section for the XeX\*( $\Omega$ ) formation generally can be expressed by

$$\sigma^{\Omega}(M_j') = \sigma_{\Omega'=\Omega}^{\Omega} \times W_{\Omega'=\Omega}(M_j') + \sigma_{\Omega' \neq \Omega}^{\Omega} \times W_{\Omega' \neq \Omega}(M_j') \quad (8)$$

where  $\sigma_{\Omega'=\Omega}^{\Omega}$  is the cross section for the  $\Omega' = \Omega$  case (i.e., XeX\*( $\Omega$ ) formation from the configuration of Xe<sup>+</sup> ( $^2P_{3/2}$ ,  $\Omega' = \Omega$ ) in the collision frame) and  $\sigma_{\Omega' \neq \Omega}^{\Omega}$  is the cross section for the  $\Omega' \neq \Omega$  case (i.e., XeX\*( $\Omega$ ) formation from the configuration of Xe<sup>+</sup> ( $^2P_{3/2}$ ,  $\Omega' \neq \Omega$ ) in the collision frame). In this case, we can express  $\sigma_{\Omega'=\Omega}^{\Omega}$  and  $\sigma_{\Omega' \neq \Omega}^{\Omega}$  by the following relationship

$$\sigma^{M_j'=2}(\Omega) = \sigma_{\Omega'=3/2}^{\Omega}, \quad \sigma^{M_j'=1}(\Omega) = 0.25 \times \sigma_{\Omega'=3/2}^{\Omega} + 0.75 \times \sigma_{\Omega'=1/2}^{\Omega}, \quad \sigma^{M_j'=0}(\Omega) = \sigma_{\Omega'=1/2}^{\Omega}$$

Therefore,  $A^{M_j'=2}$  corresponds to the rotational alignment for the  $\Omega' = 3/2$  case, whereas  $A^{M_j'=0}$  corresponds to that for the  $\Omega' = 1/2$  case. From Figure 3, it is found that the rotational alignment for the  $\Omega' = 1/2$  configuration ( $A^{M_j'=0}$ ) is largest for the XeX\* (B,  $\Omega = 1/2$ ) channel, whereas the  $\Omega' = 3/2$  configuration ( $A^{M_j'=2}$ ) gives the largest rotational alignment in the XeX\* (C,  $\Omega = 3/2$ ) channel. For the CCl<sub>4</sub>, the  $\Omega' = 3/2$  configuration exceptionally gives the largest rotational alignment in both the XeX\* (C) and XeX\* (B) channels. Moreover, it is found that the rotational alignment for the  $\Omega' = 3/2$  configuration ( $A^{M_j'=2}$ ) is similar in both the XeX\* (C) and XeX\* (B) channels, whereas the rotational alignment for the  $\Omega' = 1/2$  configuration ( $A^{M_j'=0}$ ) is significantly different between the XeX\* (C) and XeX\* (B) channels. These differences strongly suggest that the angular momentum  $\Omega'$  of Xe ( $^3P_2$ ,  $M_j = 2$ ) in the collision frame should make a difference on the reaction mechanism between the XeX\* (B) and XeX\* (C) channels. The  $\Omega'$  dependence can be alternatively related to the  $L_{z'}$  dependence. The similar positive rotational alignment ( $A^{M_j'=2}$ ) for the  $\Omega' = 3/2$  configuration in both the XeX\* (C) and XeX\* (B) channels is related to the similar positive alignment  $A^{L_{z'}=1}$  between the XeX\* (B) and XeX\* (C) channels (Figure 4) because the  $|L_{z'}| = 1$  configuration directly correlates with the  $\Omega' = 3/2$  configuration (i.e.,  $|\text{Xe}^+(^2P_{3/2}, \Omega' = 3/2)\rangle = |\text{Xe}^+(^2P_{3/2}, L_{z'} = 1, S_{z'} = 1/2)\rangle$ ), whereas the different rotational alignment ( $A^{M_j'=0}$ ) for the  $\Omega' = 1/2$  configuration between the XeX\* (C) and XeX\* (B) channels can be related to the difference in the alignment  $A^{L_{z'}=0}$  between the XeX\* (B) and XeX\* (C) channels (Figure 4) because the  $|L_{z'}| = 0$  configuration dominantly correlates with the  $\Omega' = 1/2$  configuration (i.e.,  $|\text{Xe}^+(^2P_{3/2}, \Omega' = 1/2)\rangle = (2/3)^{1/2} \times |\text{Xe}^+(^2P_{3/2}, L_{z'} = 0, S_{z'} = 1/2)\rangle + (1/3)^{1/2} \times |\text{Xe}^+(^2P_{3/2}, L_{z'} = 1, S_{z'} = -1/2)\rangle$ ).

According to the  $\Omega'$ -conservation model, the cross section of XeX\* ( $\Omega$ ) formation from the  $M_j'$  state at the angle  $\phi$  ( $\phi = \arcsin(b/R_{ET})$ ) can be estimated by considering the rotational coupling using the Wigner's  $d$  function,  $d_{\Omega_I, \Omega}^{3/2}(\phi)$ , as follows<sup>37</sup>

$$\sigma^{\Omega}(M_j') = [ \langle \sigma_{1/2 \rightarrow \Omega}(\phi) \times |d_{1/2, 1/2}^{3/2}(\phi)|^2 \rangle + \langle \sigma_{3/2 \rightarrow \Omega}(\phi) \times |d_{1/2, 3/2}^{3/2}(\phi)|^2 \rangle ] \times W_{1/2}(M_j') + [ \langle \sigma_{1/2 \rightarrow \Omega}(\phi) \times |d_{3/2, 1/2}^{3/2}(\phi)|^2 \rangle + \langle \sigma_{3/2 \rightarrow \Omega}(\phi) \times |d_{3/2, 3/2}^{3/2}(\phi)|^2 \rangle ] \times W_{3/2}(M_j') \quad (9)$$

where  $\sigma_{\Omega_I \rightarrow \Omega}(\phi)$  is the cross section for the XeX\*( $\Omega$ ) formation from the  $\Omega_I$  component in the ion pair (Xe<sup>+</sup>( $^2P_{3/2}$ )–RX<sup>+</sup>) frame at the angle  $\phi$  and the bracket means the averaging over the angle  $\phi$  that depends on the impact parameter ( $b$ ) distribution.

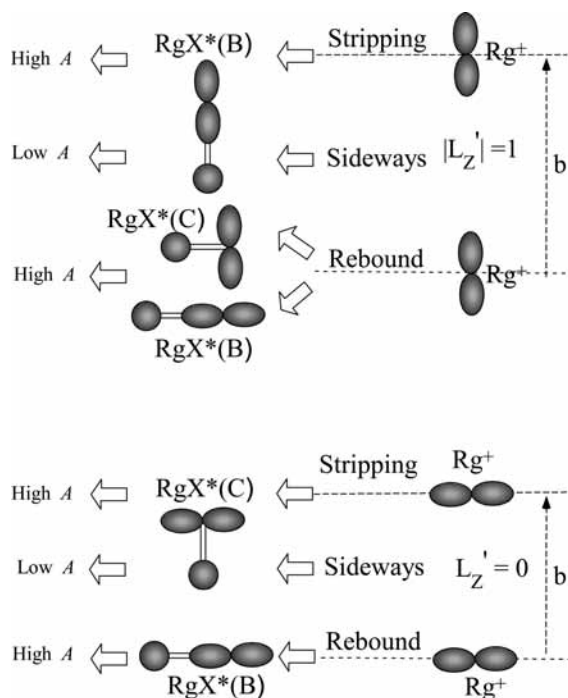


**Figure 5.** Schematic drawing of the  $L_z'$ -dependent alignment parameter  $A^{L_z'}$  and the reaction mechanism expected for each  $\text{XeX}^*$  (B, C) channel as a function of impact parameter ( $b$ ). The favorable impact parameter for each  $\text{XeX}^*$  (B, C) channel is controlled by the rotational coupling under the  $\Omega'$  conservation in the course of  $\text{XeX}^*$  (B, C) formation. The atomic alignment effect for  $\text{RgX}^*$  (C,  $\Omega = 3/2$ ) formation is controlled by the rotational coupling without considering the dynamical effect, whereas the collision with  $|L_z'| = 1$  with a small impact parameter is exceptionally reactive for the  $\text{RgX}^*$  (B,  $\Omega = 1/2$ ) formation without the conservation of the  $\Omega_1$  component in the ion-pair ( $\text{Rg}^+ - \text{RX}^-$ ) frame.

According to the rotational coupling, we can estimate the  $\Omega'$  dependence of the favorable impact parameter ( $b$ ) in the  $\text{XeX}^*$  (B,  $\Omega = 1/2$ ) and  $\text{XeX}^*$  (C,  $\Omega = 3/2$ ) channels.  $\langle |d_{\Omega', \Omega}^{3/2}(\phi)|^2 \rangle$  has a large value for  $\Omega' = \Omega_1 = \Omega$  at the small  $\phi$  (i.e., small impact parameter), whereas it has a large value for  $\Omega' \neq \Omega_1 = \Omega$  at the large  $\phi$  (i.e., large impact parameter). For the  $\text{XeX}^*$  ( $\Omega$ ) channel, the collision with  $\Omega' = \Omega$  should be favorable at the small impact parameter, whereas the collision with  $\Omega' \neq \Omega$  should be favorable at the relatively large impact parameter. For a more simple case in which the isotropic electron transfer takes place at the constant intermolecular distance  $R_{\text{ET}}$  and the straight-line trajectories with a uniform impact parameter distribution over the range from 0 to  $R_{\text{ET}}$ ,  $\langle |d_{\Omega', \Omega}^{3/2}(\phi)|^2 \rangle$  and  $\langle |d_{\Omega', \Omega_1 \neq \Omega}^{3/2}(\phi)|^2 \rangle$  have been calculated to be 0.625 and 0.375, respectively. The averaged  $\langle |d_{\Omega', \Omega}^{3/2}(\phi)|^2 \rangle$  has a maximum at  $\phi \approx 30^\circ$ , and the averaged  $\langle |d_{\Omega', \Omega_1 \neq \Omega}^{3/2}(\phi)|^2 \rangle$  has a maximum at  $\phi \approx 65^\circ$ .<sup>24</sup>

In our previous study,<sup>24</sup> it has been suggested that the atomic alignment effect for the  $\text{XeX}^*$  (C,  $\Omega = 3/2$ ) formation is dominantly controlled by the  $\Omega_1$  distribution in the ion-pair ( $\text{Xe}^+ - \text{RX}^-$ ) frame via the rotational coupling. The collisions under the  $|M_j| = 2$  ( $|L_z'| = 1$ ) configurations of  $\text{Xe}$  ( $^3\text{P}_2$ ) with the small impact parameters can produce the  $\text{XeX}^*$  (B,  $\Omega = 1/2$ ) without following the  $\Omega_1$  conservation because of the dynamical effect in the eximer formation process from the ion pair ( $\text{Xe}^+ - \text{RX}^-$ ). These situations are schematically shown in Figure 5. In addition, we have reported that the fraction of the  $\Omega_1$ -changing process in the  $\text{RgX}^*$  formation has no dependence on the reactant;  $\sigma_{1/2 \rightarrow 3/2} / \sigma^{\text{RgX}^*} \approx 0$  and  $\sigma_{3/2 \rightarrow 1/2} / \sigma^{\text{RgX}^*} = 0.375$ . According to the  $\Omega'$ -conservation model, the exceptional feature

in the  $\text{CCl}_4$  reaction can be recognized as the large contribution of the  $\Omega_1$ -changing process  $\sigma_{3/2 \rightarrow 1/2}$  in the  $\text{XeX}^*$  (B,  $\Omega = 1/2$ ) formation.

Because the reaction mechanisms of many of the alkali-halide systems have been well studied by differential scattering, it is instructive to discuss the present results in terms of these mechanisms. In general, the reaction mechanisms are classified into three types: rebound, stripping, and sideways scattering.<sup>38–42</sup> The alignment of product rotation in each mechanism can be characterized as below. A rebound mechanism is dominated by the collisions with small impact parameters, and the large repulsive energy releases between the products. Because the product's relative velocity vector  $\mathbf{k}'$  is opposed to the initial relative velocity  $\mathbf{k}$  in this mechanism, the product's angular momentum  $\mathbf{j}'$  is constrained to the preferential alignment perpendicular to  $\mathbf{k}$ , resulting in the large positive alignment. A stripping mechanism is dominated by the collisions with large impact parameters and releases small repulsive energy between the products. In this mechanism, the products with  $\mathbf{k}'$  parallel to  $\mathbf{k}$  are scattered predominantly into the forward hemisphere. As a result, a large positive alignment of  $\mathbf{j}'$  is expected. A sideways mechanism is dominated by the collisions with middle impact parameters, and the repulsive energy is released off-axis with respect to  $\mathbf{k}$ , resulting in the negative or small positive alignment due to a tipping of the reaction plane.

According to the rotational coupling, the collision with  $|L_z'| = 1$  ( $\Omega' = 3/2$ ) should be favorable at the small impact parameter for the  $\text{XeX}^*$  (C,  $\Omega = 3/2$ ) channel. Therefore, the collision with  $|L_z'| = 1$  should be favorable for the rebound mechanism and causes a high positive alignment ( $A^{L_z'=1}$ ). This type of mechanism has been known in the reactive scattering of the alkali metals by  $\text{CH}_3\text{I}$ .<sup>38–40</sup> The collision with  $L_z' = 0$  ( $\Omega' = 1/2$ ) should be favorable at relatively large impact parameter. Therefore, the collision with  $L_z' = 0$  is expected to be favorable for the sideways scattering. This mechanism should cause a low alignment  $A^{L_z'=0} \approx 0$ . As an exception,  $\text{CF}_3\text{I}$  shows a high alignment, even for the collision with  $L_z' = 0$ . This result might indicate that  $\text{XeI}^*$  (C) is produced via the stripping-type mechanism by the collisions with large impact parameters, because  $\text{CF}_3\text{I}$  has a large cross section as compared with the other reactants.<sup>16–18</sup>

For the  $\text{XeX}^*$  (B,  $\Omega = 1/2$ ) channel, the collision with  $L_z' = 0$  ( $\Omega' = 1/2$ ) should be favorable at the small impact parameter according to the rotational coupling. In this case, the rebound mechanism should be favorable and causes a large positive alignment ( $A^{L_z'=0}$ ). By way of exception,  $\text{CCl}_4$  shows no alignment for the collision with  $L_z' = 0$ . This exceptional feature might be attributed to the off-axis repulsive energy release with respect to the initial relative velocity due to the large misalignment between the ion-pair ( $\text{Xe}^+ - \text{RX}^-$ ) frame with the  $\text{XeX}^*$  axis because  $\text{CCl}_4$  has four potentially reactive sites. This might reflect the fact that the  $\text{CCl}_4$  reaction is dominated via a mechanism like the sideways mechanism because this type of mechanism has been known in the reactive scattering of the alkali metals by  $\text{CCl}_4$ .<sup>41</sup> In contrast with the  $\text{XeX}^*$  (C,  $\Omega = 3/2$ ) channel, the collision with  $|L_z'| = 1$  ( $\Omega' = 3/2$ ) is exceptionally favorable at both small and large impact parameters for the  $\text{XeX}^*$  (B,  $\Omega = 1/2$ ) channel without following the  $\Omega_1$  conservation because of the dynamical effect in the eximer formation process; that is, a high positive alignment ( $A^{L_z'=1}$ ) is possible even for the  $|L_z'| = 1$  configuration.

As a result, it is found that the  $\Omega'$ -conservation model can fairly explain the main characteristics of the  $L_z'$ -dependent alignment ( $A^{L_z'}$ ) in both the  $\text{XeX}^*$  (B) and  $\text{XeX}^*$  (C) channels.

In other words, the difference in the alignment ( $A^{Lz'}$ ) between the XeX\* (B) and XeX\* (C) channels can be recognized as the change of reaction mechanism due to the difference in the favorable impact parameter for each  $M_J'$  state between the XeX\* (B) and XeX\* (C) channels, which reflects the  $\Omega'$  conservation in the course of ion-pair ( $\text{Rg}^+-\text{RX}^-$ ) formation.

#### 4. Conclusions

For the reactions of oriented Xe\* ( $^3\text{P}_2$ ,  $M_J = 2$ ) + halogen (X)-containing molecules ( $\text{CCl}_4$ ,  $\text{CF}_3\text{Br}$ ,  $\text{CF}_3\text{I}$ ,  $\text{CH}_3\text{I}$ ,  $\text{NF}_3$ ), the alignment ( $A^{M_J'}$ ) of the XeX\* (B, C) rotations has been measured as a function of each magnetic  $M_J'$  substate in the collision frame. The correlation between the atomic alignment ( $M_J'$ ) and the alignment ( $A^{M_J'}$ ) of the XeX\* (B, C) rotations is found to be extremely different between the XeX\* (B) and XeX\* (C) channels. (For XeX\* (B),  $A^{M_J'}$  is highest for the  $M_J' = 0$  state, except  $\text{CCl}_4$ , whereas the  $|M_J'| = 2$  states give the highest  $A^{M_J'}$  for XeX\* (C).) The correlation between the configuration ( $L_Z'$ ) of the inner 5p orbital and the  $L_Z'$ -dependent alignment ( $A^{L_Z'}$ ) of the XeX\* (B, C) rotations is also revealed. For XeX\* (C), the  $L_Z' = 0$  configuration causes no alignment (i.e.,  $A^{L_Z'} \approx 0$ ) except  $\text{CF}_3\text{I}$ , and only the  $|L_Z'| = 1$  configuration induces the alignment  $A^{L_Z'}$  of the XeX\* (C) rotation. In contrast with XeX\* (C), both the  $|L_Z'| = 1$  and  $L_Z' = 0$  configurations cause the alignment  $A^{L_Z'}$  of the XeX\* (B) rotation. The difference in the alignment ( $A^{L_Z'}$ ) between the XeX\* (B) and XeX\* (C) channels can be recognized as the change of reaction mechanism because of the difference of favorable impact parameters for each  $M_J'$  state between the XeX\* (B) and XeX\* (C) channels if the  $\Omega'$  is conserved in the course of ion-pair ( $\text{Rg}^+-\text{RX}^-$ ) formation. That is, the present study confirms the proposal that the  $\Omega'$  component in the collision frame is really conserved in the course of  $\text{RgX}^*$  formation.

#### References and Notes

- (1) Brooks, P. R. *Science* **1976**, *193*, 11.
- (2) Parker, D. H.; Bernstein, R. B. *Annu. Rev. Phys. Chem.* **1989**, *40*, 561.
- (3) Bulthuis, J.; van Leuken, J. J.; Stolte, S. *J. Chem. Soc., Faraday Trans.* **1995**, *91*, 205.
- (4) de Vries, M. S.; Srdanov, V. I.; Hanrahan, C. P.; Maetin, R. M. *J. Chem. Phys.* **1983**, *78*, 5582.
- (5) Karny, Z.; Estler, R. C.; Zare, R. N. *J. Chem. Phys.* **1978**, *69*, 5199.
- (6) Simpson, W. R.; Rakitzis, T. P.; Kandel, S. A.; Orr-Ewing, A. J.; Zare, R. N. *Stereodynamics and Active Control in Chemical Reactions*; CNRS: Gif-sur-Yvette, France, 1994; p 2.
- (7) Loesch, H. J.; Remscheid, A. *J. Chem. Phys.* **1990**, *93*, 4779.
- (8) Friedrich, B.; Herschbach, D. R. *Z. Phys. D* **1991**, *18*, 153.

- (9) Cappelletti, D.; Pirani, F.; Scotoni, M.; Demarchi, G.; Vattuone, L.; Gerbi, A.; Rocca, M. *Eur. Phys. J. D* **2006**, *38*, 121.
- (10) Brooks, R. B. *J. Chem. Phys.* **2009**, *130*, 151102.
- (11) Rettner, C. T.; Zare, R. N. *J. Chem. Phys.* **1982**, *77*, 2416.
- (12) Yang, W. S.; Ding, G. W.; Xu, D. L.; Sun, W. Z.; Gu, Y. S.; He, G. Z.; Lou, N. Q. *Chem. Phys.* **1995**, *193*, 345.
- (13) Suits, A. G.; Hou, H.; Davis, H. F.; Lee, Y. T. *J. Chem. Phys.* **1992**, *96*, 2777.
- (14) Han, K. L.; Zhang, L.; Xu, D. L.; He, G. Z.; Lou, N. Q. *J. Phys. Chem. A* **2001**, *105*, 2956.
- (15) Riley, S. J.; Siska, P. E.; Herschbach, D. R. *Faraday Discuss. Chem. Soc.* **1979**, *67*, 27.
- (16) Tamagake, K.; Setser, D. W.; Kolts, J. H. *J. Chem. Phys.* **1981**, *74*, 4286.
- (17) Kolts, J. H.; Velazco, J. E.; Setser, D. W. *J. Chem. Phys.* **1979**, *71*, 1247.
- (18) Sadeghi, N.; Cheaib, M.; Setser, D. W. *J. Chem. Phys.* **1989**, *90*, 219.
- (19) Zhong, D.; Setser, D. W.; Sobczynski, R.; Gadomski, W. *J. Chem. Phys.* **1996**, *105*, 5020.
- (20) Velazco, J. E.; Kolts, J. H.; Setser, D. W. *J. Chem. Phys.* **1976**, *65*, 3468.
- (21) Tsuji, M.; Furusawa, M.; Nishimura, Y. *J. Chem. Phys.* **1990**, *92*, 6502.
- (22) Hay, P. J.; Dunning, T. H., Jr. *J. Chem. Phys.* **1978**, *69*, 2209.
- (23) Yasuda, K.; Ohoyama, H.; Kasai, T. *J. Phys. Chem. A* **2008**, *112*, 11543.
- (24) Ohoyama, H.; Yasuda, K.; Kasai, T. *J. Phys. Chem. A* **2009**, in press.
- (25) Orr-Ewing, A. J.; Zare, R. A. *Annu. Rev. Phys. Chem.* **1994**, *45*, 315.
- (26) Zhang, W.; Cong, S.; Zhang, C.; Xu, X.; Chen, M. *J. Phys. Chem. A* **2009**, *113*, 4192.
- (27) Case, D. A.; Herschbach, D. R. *Mol. Phys.* **2002**, *100*, 109.
- (28) Jalink, H.; Parker, D. H.; Stolte, S. *J. Chem. Phys.* **1986**, *85*, 5372.
- (29) Jalink, H.; Nicolaesens, G.; Stolte, S.; Parker, D. H. *J. Chem. Soc., Faraday Trans. 2* **1989**, *85*, 1115.
- (30) Engelke, F.; Meiwes-Broer, K. H. *Chem. Phys. Lett.* **1984**, *108*, 132.
- (31) Costen, M. L.; Hancock, G.; Orr-Ewing, A. J.; Summerfield, D. *J. Chem. Phys.* **1994**, *100*, 2754.
- (32) Brouard, M.; Duxon, S. P.; Enriquez, P. A.; Simons, J. P. *J. Phys. Chem.* **1991**, *95*, 8169.
- (33) Zhan, J. P.; Yang, H. P.; Han, K. L.; Deng, W. Q.; He, G. Z.; Lou, N. Q. *J. Phys. Chem. A* **1997**, *101*, 7486.
- (34) Tyndall, G. W.; de Vries, M. S.; Cobb, C. L.; Martin, R. M. *Chem. Phys. Lett.* **1992**, *195*, 279.
- (35) Watanabe, D.; Ohoyama, H.; Matsumura, T.; Kasai, T. *J. Chem. Phys.* **2006**, *125*, 084316.
- (36) Watanabe, D.; Ohoyama, H.; Matsumura, T.; Kasai, T. *Phys. Rev. Lett.* **2007**, *99*, 043201.
- (37) Zare, R. N. *Angular Momentum*; Wiley: New York, 1998.
- (38) Rulis, A. M.; Bernstein, R. B. *J. Chem. Phys.* **1972**, *57*, 5497.
- (39) Herschbach, D. R. *Faraday Discuss. Chem. Soc.* **1973**, *55*, 233.
- (40) Gordon, R. J.; Herm, R. R.; Herschbach, D. R. *J. Chem. Phys.* **1968**, *49*, 2684.
- (41) Hijazi, N. H.; Polanyi, J. C. *J. Chem. Phys.* **1975**, *63*, 2249.
- (42) Wilson, K. R.; Herschbach, D. R. *J. Chem. Phys.* **1968**, *49*, 2676.

JP906388V